

# Surface Potential Fluctuations of SiO<sub>2</sub>/SiC Interfaces Investigated by Local Capacitance-Voltage Profiling Based on Time-Resolved Scanning Nonlinear Dielectric Microscopy

Kohei Yamasue<sup>a\*</sup> and Yasuo Cho<sup>b</sup>

Tohoku University, 2-1-1 Katahira, Aoba, Sendai, Miyagi 980-8577, Japan

<sup>a</sup>yamasue@riec.tohoku.ac.jp, <sup>b</sup>yasuocho@riec.tohoku.ac.jp

**Keywords:** SiC-MOSFET, Interface defects, Scanning nonlinear dielectric microscopy, Surface potential fluctuations, Local capacitance-voltage profiling

**Abstract.** We investigate surface potential fluctuations on SiO<sub>2</sub>/SiC interfaces by local capacitance-voltage profiling based on time-resolved scanning nonlinear dielectric microscopy. As experimental indicators of surface potential fluctuations, we measured the spatial fluctuations of local capacitance-voltage and its first derivative profiles through the detection of the voltages at the inflection points of the profiles. We show that, even for a sample with a nitrated interface with low interface defect density, the fluctuations of the measured voltages are much higher than the thermal energy at room temperature. This indicates the existence of high potential fluctuations, which can give a significant impact on the carrier transport at the SiO<sub>2</sub>/SiC interface of SiC metal-oxide-semiconductor field effect transistors.

## Introduction

SiO<sub>2</sub>/SiC interfaces have been extensively studied because of their significant impact on the performance of the SiC metal-oxide-semiconductor field effect transistors (MOSFETs) such as channel mobility and threshold voltage [1, 2]. Si-face 4H-SiC MOSFETs with an as-oxidized MOS interface typically show a peak field effect mobility ( $\mu_{FE}$ ) of  $\sim 10$  cm<sup>2</sup>/Vs or less. As a standard treatment, post oxidation annealing (POA) in nitrogen rich environments has been established for the reduction of interface defect density ( $D_{it}$ ) [3-7]. Although the POA treatment improves the peak of  $\mu_{FE}$  (e.g. POA in NO achieves about 40 cm<sup>2</sup>/Vs), the achievable mobility is still much lower than the bulk mobility in SiC. In order to understand the cause of the observed low mobility, possible mechanisms have been suggested so far [8, 9]. In addition, recently, the formation of the interface by hydrogen etching pretreatment of a SiC surface followed by SiO<sub>2</sub> deposition instead of thermal oxidation has been proposed and paid considerable attention as a key to further drastic reduction of interface defects including those at shallow levels [10]. It has been demonstrated that this new technique allows the fabrication of normally-off transistors with  $\mu_{FE}$  of  $\sim 80$  cm<sup>2</sup>/Vs at the peak [11]. However, the record value is still one order magnitude lower than bulk carrier mobility of SiC (1000 cm<sup>2</sup>/Vs).

For deeper understanding of the interface properties, we focus on surface potential fluctuations on SiO<sub>2</sub>/SiC interfaces. An early study using the conductance method by Bano *et al.* has shown that, unlike SiO<sub>2</sub>/Si, SiO<sub>2</sub>/SiC interfaces have surface potential fluctuations largely exceeding the thermal energy at room temperature ( $\sim 26$  mV) [12]. It has been pointed out that the high surface potential fluctuations can give a significant impact on the carrier transport at the SiO<sub>2</sub>/SiC interfaces [12, 13]. Thus, here we investigate the surface potential fluctuations at the SiO<sub>2</sub>/SiC interfaces by scanning nonlinear dielectric microscopy (SNDM) [14]. SNDM is a scanning probe microscopy method that has exceptionally high sensitivity to the variation in the microscopic capacitance. So far, the imaging the first voltage derivative of capacitance ( $dC/dV$ ) by the conventional SNDM was performed on various SiO<sub>2</sub>/SiC samples. It has been shown that the  $dC/dV$  images for the samples with different macroscopic  $D_{it}$  levels have commensurate levels of spatial fluctuations [15]. The fluctuations of  $dC/dV$  reflect those of local CV profiles in part. If the local CV profiling is enabled, we are able to give real-space microscopic insights on the surface potential fluctuations of the SiO<sub>2</sub>/SiC interfaces.

In this paper, we perform local CV profiling on SiO<sub>2</sub>/SiC based on recently developed time-resolved SNDM (tr-SNDM). We discuss the spatial fluctuation of local CV profiles in real-space by extracting the voltages giving particular features of the profiles. We show that the fluctuations of the extracted voltages are much higher than the thermal energy at room temperature.

### Local CV and $dC/dV$ - $V$ Profiling

Local CV profiling was here performed using tr-SNDM [16]. A tr-SNDM setup was implemented to a commercial atomic force microscopy (AFM) system (Bruker, Dimension Icon) operated in air at room temperature. We mounted a lab-made SNDM probe on the AFM head; the SNDM probe is made of an LC self-oscillator and detects the variation in the microscopic capacitance below the conductive tip of an AFM cantilever attached to the oscillator. The center frequency of the oscillator is modulated by the capacitance variation caused by a voltage pulse applied between the tip and sample. Unlike the conventional SNDM using classical analog signal processing, tr-SNDM demodulates the capacitance response to the voltage pulse by the high-speed direct digitization and offline software signal processing. This permits wide measurement bandwidth and flexible signal treatments. The more details of the technique and setup can be found in Ref. [16].

We can perform point-by-point local CV and  $dC/dV$ - $V$  profiling by sweeping the voltage at each measurement point on the sample [17, 18]. When a triangular voltage pulse is used for the voltage sweep, the resulting capacitance response can be converted to backward and forward local CV profiles over the sweep range [17]. In addition, the first derivative of the local CV profile, or a  $dC/dV$ - $V$  profile, can be simultaneously taken by adding a small high frequency voltage to the triangular pulse [18]. The  $dC/dV$ - $V$  profile can be obtained from a high frequency component arising in the capacitance response, because it has a higher amplitude as the slope of the local CV profile increases. The local CV profiling performed here differs from the standard macroscopic CV profiling based quasi-static voltage sweep. The sweep rate in the local CV profiling is typically equivalent to the frequency in the order of 10 kHz and thus the profiles reflect deep depletion in the depletion region, since an inversion layer is not formed during the fast voltage sweep.

In order to discuss the spatial fluctuations of the local CV profiles, here we focus on the fluctuations of the voltages at the inflection points of the individual local CV and  $dC/dV$ - $V$  profiles. As shown in Fig. 1, these voltages are here denoted  $V_1$  and  $V_2$ .  $V_1$  and  $V_2$  respectively denote the voltage at the inflection point of a local CV profile and that of the corresponding  $dC/dV$ - $V$  profile. We extract  $V_1$  and  $V_2$  to estimate the voltage shifts of the local CV profiles.  $V_1$  and  $V_2$  are numerically detected by finding the voltage at the negative peak of a local  $dC/dV$ - $V$  profile and that at the positive peak of a local  $d^2C/dV^2$ - $V$  profile, respectively. Local  $d^2C/dV^2$ - $V$  profiles are numerically derived from the  $dC/dV$ - $V$  profiles. The fluctuations of  $V_1$  and  $V_2$  are experimental indicators for surface potential fluctuations, because the fluctuations of a built-in potential at the interface causes the shift of the local CV profiles. The fluctuations can be caused by the spatially non-uniform distribution of  $D_{it}$  and fixed oxide charge density at the interface.  $V_1$  and  $V_2$  can have different spatial distributions, because they reflect the different spatial distributions of charge states at the different energy levels in general. Since  $V_2$  is located closer to the deep depletion region, the spatial fluctuations of  $V_2$  are dominated by those of the static charge states with no significant dependence on the applied voltage such as fixed oxide charges and deep level defects. The fluctuations of  $V_1$  located near the accumulation region are further affected by those of voltage-dependent charge states such as defects at shallower levels. This implies that  $V_1$  is expected to be higher than  $V_2$ , as the fluctuations of  $V_1$  are cumulatively affected from the shallower levels as well as the static interface charge states.

It is noted that similar local CV analysis, called scanning capacitance spectroscopy [19], has also been performed for SiO<sub>2</sub>/4H-SiC samples by scanning capacitance microscopy [20]. In Ref. [20], local CV profiles were obtained by integrating  $dC/dV$ - $V$  profiles to discuss the spatial fluctuations of  $V_1$ , while the sweep rate was much smaller than that in this study.

## Results and Discussions

Here we measured local CV and  $dC/dV$ - $V$  profiles on two different n-type 4H-SiC(0001) samples with a 10 nm-thick thermal oxide layer and  $10^{16} \text{ cm}^{-3}$  dopant concentration. One of the samples was as-oxidized but the other was further treated by POA in NO gas for 60 min. at 1250 deg. C. The oxide layers of the measured samples were thinner than those of typical SiC wafers for power device applications in order to obtain higher spatial resolution in local CV profiling. We think that even the samples with such a thin oxide layer are worth investigating. This is because, as reported in Refs. [21, 22], electric defects such as interface defects, oxide charges, and near interface traps have been detected even for SiC with thin oxide layer thickness, while their density depends on the thickness. In addition, it has been considered that nitrogen atoms are localized at the  $\text{SiO}_2/\text{SiC}$  interface treated by POA in NO gas [23, 24].

We used a Pt-Ir coated microcantilever with a 100 nm radius tip (NanoWorld, EFM-100). For local CV profiling, we applied a 1.5 cycle triangular voltage pulse with an amplitude of 20 V<sub>pp</sub> and a slew rate of 0.4 V/ $\mu\text{s}$ . In addition, a 1 MHz and 2 V<sub>pp</sub> high frequency sinusoidal voltage was added to the triangular pulse for the simultaneous  $dC/dV$ - $V$  profiling. The voltage was applied to the sample relative to the grounded tip. For the reduction of noise, a local CV profile was obtained by averaging the capacitance responses to repetitive 160 voltage pulses at each measurement point. The scan size was 1  $\mu\text{m} \times 1 \mu\text{m}$  for both samples.

Figure 2 shows typical local CV [Fig. 2(a)] and  $dC/dV$ - $V$  [Fig. 2(b)] profiles for the as-oxidized sample. It is confirmed that the local CV profiles showed typical n-type characteristics with a negative slope. As shown in Fig. 3, the nitrided sample had local CV and  $dC/dV$ - $V$  profiles less stretched out than the as-oxidized one, which was expected from the significant reduction of  $D_{it}$  by the POA treatment. Figures 4 and 5 show  $V_1$  and  $V_2$  images for the as-oxidized and nitrided samples, respectively. The images were reconstructed by extracting  $V_1$  and  $V_2$  values from the backward and forward local CV and  $dC/dV$ - $V$  profiles. We found that  $V_1$  and  $V_2$  had spatially non-uniform clustered distributions as similar to  $dC/dV$  reported in the previous study [15]. The standard deviations (SDs) of  $V_1$  and  $V_2$  were summarized in Table I for the comparison of fluctuations. For obtaining  $V_1$  values, outliers were excluded, because  $V_1$  was not detected within the measurement range on some measurement points especially for the as-oxidized sample. The SDs of  $V_1$  were as high as 1 V for the as-oxidized sample but decreased by 80 % for the nitrided sample, which indicates the POA treatment significantly reduces  $D_{it}$  contributing surface potential fluctuations.  $V_2$  less fluctuated than  $V_1$  for both samples, as expected from the location of  $V_2$  closer to the deep depletion region with lower interface charge density. The SDs of  $V_2$  also decreased by 40 % through the POA treatment and became lowest but still several times higher than the thermal energy at room temperature. This suggest that the elimination of the static interface charges and their fluctuations is at least necessary to suppress surface potential fluctuations within the thermal energy level.

## Conclusion

We performed local CV profiling on the as-oxidized and nitrided  $\text{SiO}_2/\text{SiC}$  samples for investigating the surface potential fluctuations, which may give a significant impact on the carrier transport properties of SiC MOSFETs. The SDs of  $V_1$  and  $V_2$  largely exceeded the thermal energy at room temperature even for the nitrided sample. Our results indicate that surface potential fluctuations remain high even after the significant reduction of  $D_{it}$  by the POA treatment. It seems that the surface potential fluctuations are already higher than the thermal energy due to the contribution of the static interface charge states such as fixed charges and deep level defects and they further increase with the charge trapping to shallower levels.

## Acknowledgements

We thank Dr. Hajime Okumura and his group of National Institute of Advanced Industrial Science and Technology for providing  $\text{SiO}_2/\text{SiC}$  samples and macroscopic evaluation results. We also thank

Mr. Toshihiko Iwai, Tohoku University, Japan, for the development of SNDM probes. We are grateful for the experimental assistance given by Ms. Tamiko Ambo, Tohoku University, Japan. This work was supported in part by Grant-in-Aid for Scientific Research (S) (Grant No. 16H06360) from the Japan Society for the Promotion of Science.

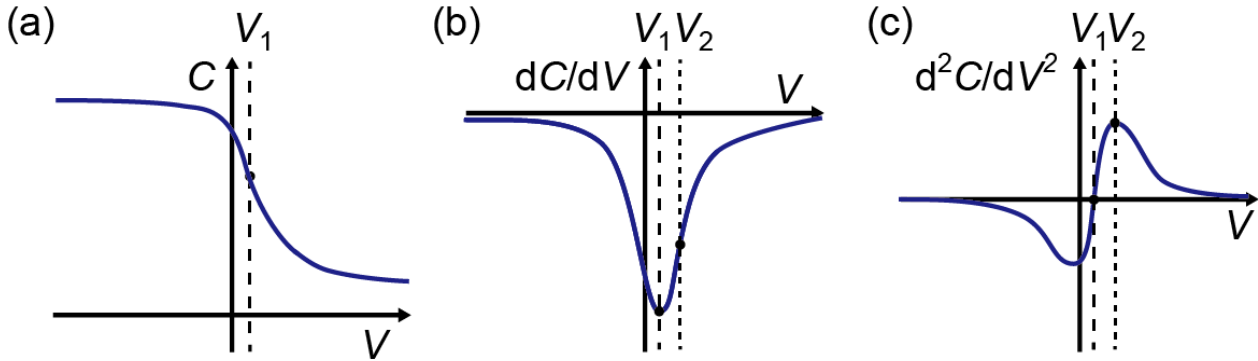


Fig. 1. Schematic illustration of local CV [(a)],  $dC/dV$ - $V$  [(b)], and  $d^2C/dV^2$ - $V$  profile [(c)] for an n-type local metal-insulator-semiconductor capacitor.  $V_1$  and  $V_2$  respectively denote the voltage at the inflection point in (a) and that in (b).

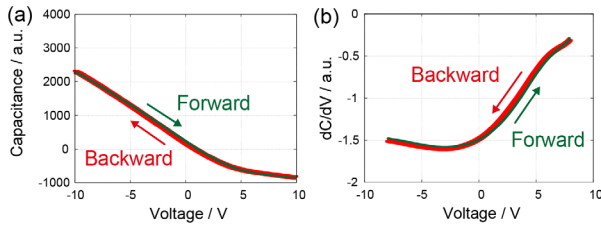


Fig. 2. Typical local (a) CV and (b)  $dC/dV$ - $V$  profiles of the as-oxidized  $\text{SiO}_2/\text{SiC}$  sample

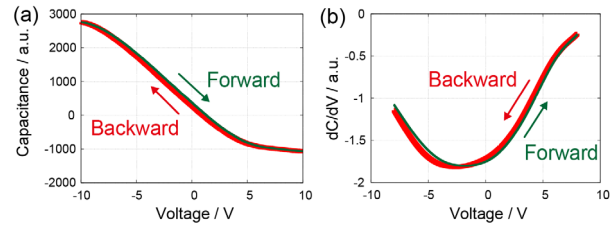


Fig. 3. Typical local (a) CV and (b)  $dC/dV$ - $V$  profiles of the nitrated  $\text{SiO}_2/\text{SiC}$  sample

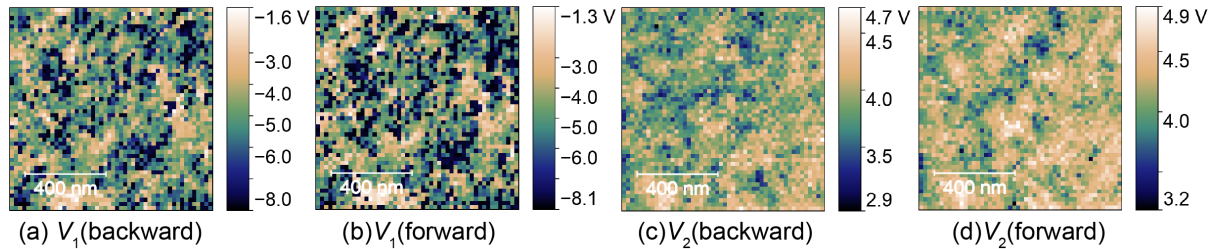


Fig. 4.  $V_1$  and  $V_2$  images of the as-oxidized sample.

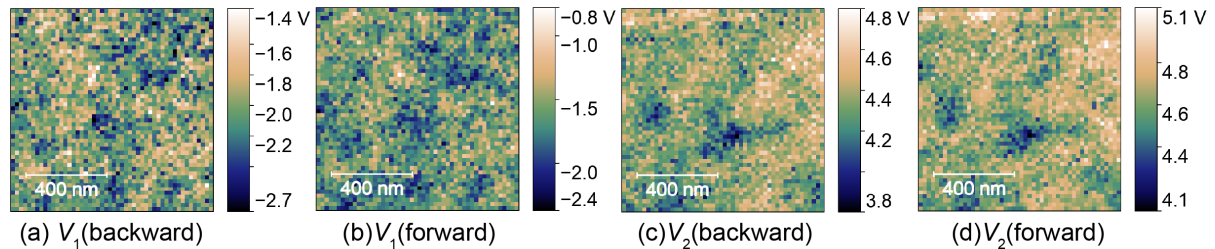


Fig. 5.  $V_1$  and  $V_2$  images of the nitrated sample.

Table I. Standard deviations of fluctuations in  $V_1$  and  $V_2$

Sample	$V_1$ (backward) / V	$V_1$ (forward) / V	$V_2$ (backward) / V	$V_2$ (forward) / V
As-oxidized	1.01	1.12	0.25	0.24
Nitrated	0.22	0.22	0.14	0.13

## References

- [1] V. V. Afanasev, M. Bassler, G. Pensl, and M. Schulz, Intrinsic SiC/SiO<sub>2</sub> Interface States, *Phys. Status Solidi (a)* 162 (1997) 321-337.
- [2] T. Kimoto, Material science and device physics in SiC technology for high-voltage power devices, *Jpn. J. Appl. Phys.* 54 (2015) 040103.
- [3] H. Li, S. Dimitrijević, H.B. Harrison, and D. Sweatman, Interfacial characteristics of N<sub>2</sub>O and NO nitrided SiO<sub>2</sub> grown on SiC by rapid thermal processing, *Appl. Phys. Lett.* 70 (1997) 2028.
- [4] G. Y. Chung, C. C. Tin, J. R. Williams, K. McDonald, R. K. Chanana, R. A. Weller, S. T. Pantelides, L. C. Feldman, O. W. Holland, M. K. Das, and J. W. Palmour, Improved Inversion Channel Mobility for 4H-SiC MOSFETs Following High Temperature Anneals in Nitric Oxide, *IEEE Electron Device Lett.* 22 (2001) 176-178.
- [5] M. Noborio, J. Suda, S. Beljakowa, M. Krieger, and T. Kimoto, 4H-SiC MISFETs with nitrogen-Containing Insulators, *Phys. Status Solidi (a)* 206 (2009) 2374.
- [6] P. Fiorenza, F. Giannazzo, and F. Roccaforte, Characterization of SiO<sub>2</sub>/4H-SiC Interfaces in 4H-SiC MOSFETs: A Review, *Energies* 12 (2019) 2310.
- [7] T. Kimoto and H. Watanabe, Defect engineering in SiC technology for high-voltage power devices, *Appl. Phys. Express* 13 (2020) 120101.
- [8] Y. Matsushita and A. Oshiyama, A Novel Intrinsic Interface State Controlled by Atomic Stacking Sequence at Interfaces of SiC/SiO<sub>2</sub>, *Nano Lett.* 17 (2017) 6458-6463.
- [9] M. Sometani, T. Hosoi, H. Hirai, T. Hatakeyama, S. Harada, H. Yano, T. Shimura, H. Watanabe, Y. Yonezawa, and H. Okumura, Ideal phonon-scattering-limited mobility in inversion channels of 4H-SiC(0001) MOSFETs with ultralow net doping concentrations, *Appl. Phys. Lett.* 115 (2019), 132102.
- [10] K. Tachiki, M. Kaneko, T. Kobayashi, and T. Kimoto, Formation of high-quality SiC(0001)/SiO<sub>2</sub> structures by excluding oxidation process with H<sub>2</sub> etching before SiO<sub>2</sub> deposition and high-temperature N<sub>2</sub> annealing, *Appl. Phys. Express.* 13 (2020) 121002.
- [11] K. Tachiki, M. Kaneko, and T. Kimoto, Mobility improvement of 4H-SiC (0001) MOSFETs by a three-step process of H<sub>2</sub> etching, SiO<sub>2</sub> deposition, and interface nitridation, *Appl. Phys. Express.* 14 (2021) 031001.
- [12] E. Bano, T. Ouisse, L. Di Cioccio, and S. Karmann, Surface potential fluctuations in metal-oxide-semiconductor capacitors fabricated on different silicon carbide polytypes, *Appl. Phys. Lett.* 65 (1994) 2723-2724.
- [13] S. Swandono, A. Penumatcha, and J.A. Cooper, Electrical Evidence of Disorder at the SiO<sub>2</sub>/4H-SiC MOS Interface and its Effect on Electron Transport, in 70th Device Research Conference, 2012, 167-168.
- [14] Y. Cho, A. Kirihaara, and T. Saeki, Scanning nonlinear dielectric microscope, *Rev. Sci. Instrum.* 67 (1996) 2297-2303.
- [15] N. Chinone, A. Nayak, R. Kosugi, Y. Tanaka, S. Harada, H. Okumura, and Y. Cho, Evaluation of silicon- and carbon-face SiO<sub>2</sub>/SiC MOS interface quality based on scanning nonlinear dielectric microscopy, *Appl. Phys. Lett.* 111 (2017) 061602.
- [16] Y. Yamagishi and Y. Cho, Nanosecond microscopy of capacitance at SiO<sub>2</sub>/4H-SiC interfaces by time-resolved scanning nonlinear dielectric microscopy, *Appl. Phys. Lett.* 111 (2017) 163103.

- 
- [17] K. Suzuki, K. Yamasue, and Y. Cho, A Study on Evaluation of Interface Defect Density on High- $\kappa$ /SiO<sub>2</sub>/Si and SiO<sub>2</sub>/Si Gate Stacks using Scanning Nonlinear Dielectric Microscopy, in 2019 IEEE International Integrated Reliability Workshop (IIRW), 2019.
- [18] K. Yamasue and Y. Cho, Local Capacitance-Voltage Profiling and Deep Level Transient Spectroscopy of SiO<sub>2</sub>/SiC Interfaces by Scanning Nonlinear Dielectric Microscopy, in the 28th edition of the IEEE International Symposium on the Physical and Failure Analysis of Integrated Circuits (IPFA 2021), 2021.
- [19] H. Edwards, R. McGlothlin, R. San Martin, E. U. M. Gribelyuk, R. Mahaffy, C. Ken Shih, R.S. List, and V.A. Ukraintsev, Scanning capacitance spectroscopy: An analytical technique for pn-junction delineation in Si devices, *Appl. Phys. Lett.* 72 (1998) 698.
- [20] P. Fiorenza, S. Di Franco, F. Giannazzo, and F. Roccaforte, Nanoscale probing of the lateral homogeneity of donors concentration in nitridated SiO<sub>2</sub>/4H-SiC interfaces, *Nanotechnology* 27 (2016) 315701.
- [21] H. Watanabe, T. Hosoi, T. Kirino, Y. Kagei, Y. Uenishi, A. Chanthaphan, A. Yoshigoe, Y. Teraoka, and T. Shimura, Synchrotron X-Ray photoelectron spectroscopy study on thermally grown SiO<sub>2</sub>/4H-SiC(0001) interface and its correlation with electrical properties, *Appl. Phys. Lett.* 99 (2011) 021907.
- [22] X. Zhang, D. Okamoto, T. Hatakeyama, M. Sometani, S. Harada, N. Iwamuro, and H. Yano, Impact of oxide thickness on the density distribution of near-interface traps in 4H-SiC MOS capacitors, *Jpn. J. Appl. Phys.* 57 (2018) 06KA04.
- [23] P. Tanner, S. Dimitrijević, H.-F. Li, D. Sweatman, K.E. Prince, and H.B. Harrison, SIMS Analysis of Nitrided Oxides Grown on 4H-SiC, *J. Electron. Mater.* 28 (1999) 109.
- [24] K. Moges, M. Sometani, T. Hosoi, T. Shimura, S. Harada, and H. Watanabe, Sub-nanometer-scale depth profiling of nitrogen atoms in SiO<sub>2</sub>/4H-SiC structures treated with NO<sub>2</sub> Annealing, *Appl. Phys. Express* 11 (2018) 101303.